Applied Thermal Engineering 133 (2018) 283–297

Contents lists available at ScienceDirect

Applied Thermal Engineering

journal homepage: www.elsevier.com/locate/apthermeng

Research Paper

Taguchi optimization of solar thermal and heat pump combisystems under five distinct climatic conditions

Yueh-Heng Li [a,b,*], Wei-Chun Kao [a]

[a] Department of Aeronautics and Astronautics, National Cheng Kung University, Tainan 701, Taiwan, ROC
[b] Research Center for Energy Technology and Strategy, National Cheng Kung University, Tainan 701, Taiwan, ROC

HIGHLIGHTS

- TRNSYS software is to simulate the solar collect and heat pump combisystem.
- Two modes of SDHW system are numerically discussed in five cities.
- The flow rate of the heat pump was most influential in single-tank system.
- The flow rate of the solar collector was most influential in dual-tank system.
- The payback periods and operating costs in the five cities were determined.

ARTICLE INFO

Article history:
Received 30 August 2017
Revised 6 December 2017
Accepted 1 January 2018

Keywords:
Solar collector
Air source heat pump
TRNSYS
Combisystem
Domestic hot water
Payback period

ABSTRACT

Solar domestic hot water systems worldwide generally combine solar collectors and heat pumps. The utilization of heat pump as the auxiliary heat generator of solar combisystem is a common solution of the last decade. Atmospheric factors such as solar radiation, ambient temperature, and relative humidity influence the performance of such systems; therefore, optimizing the flow rates in the solar and heat pump loops, as well as the volume of the water tanks, is essential to obtain maximum heating performance. In this study, the Taguchi method was applied to determine the optimal operating parameters for two solar combisystems (single- and dual-tank) by determining the higher-the-better characteristics of the signal-to-noise ratio. Moreover, five metropolitan areas were selected to investigate the effect of divergent climatic conditions on the Taguchi optimizations. The results demonstrated that the predominant parameter affecting performance varied for the two hydraulic layouts, but was identical across the five cities. In addition, the payback periods of the solar combisystems in the five cities were investigated. The combined results provide practical guidelines for choosing the best type of solar combisystem to implement under varying climatic and economic conditions.

1. Introduction

The enormous consumption of fossil fuels has deteriorated environmental conditions and eradicated species on an unprecedented scale. The soaring carbon dioxide concentration in the atmosphere is a warning for humankind. It is impossible to abandon fossil fuels altogether and maintain an identical modern lifestyle. Nevertheless, it is practical to complement fossil fuels as they deplete with sustainable renewable energy.

Solar combisystems used for space heating [1] and domestic hot water [2] present one example of a method for mitigating fossil fuel dependence. They offer the advantages of lower energy consumption [3], lower electric consumption, and higher overall efficiency [4], compared with other renewable energy technologies. Several studies have assessed the technical, economical, and environmental aspects of implementing solar combisystems. For the thermal application, an indirect expansion solar-assisted heat pump was studied and discussed the influence of various operating parameters in solar water heating and solar heating modes [5]. Carbonell et al. [6] used TRNSYS-17 and POLYSUN-6 to simulate the system performance of the combined solar thermal and heat pump system with the discrepancies of 4% for air source based system and 14% for ground source based system. Kuang and Wang [7] works on the long-term performance of a direct expansion solar assisted heat pump system for space heating in winter and air conditioning in summer and hot water during the whole year. In

* Corresponding author at: Department of Aeronautics and Astronautics, National Cheng Kung Univ., Tainan 701, Taiwan, ROC.
E-mail address: yueheng@mail.ncku.edu.tw (Y.-H. Li).

https://doi.org/10.1016/j.applthermaleng.2018.01.002
1359-4311/

addition, geothermal energy is increasing being used to heat and cool building. Galgaro et al. [8] investigated that the system performance of geoexchange systems coupled with Borehole heat exchangers in anomalous geothermal zones. Lim et al. [9] presented annual heating performance of ground source heat pump system with heat pipe (HP-GSHP) in a residential application in three different cities. Dai et al. [10] employed TRNSYS software to optimize the heating performance of solar collectors combined with a carbon dioxide heat pump. Panaras et al. [11] investigated the performance of a combined solar thermal heat pump hot water system, and they found that using the heat pump as an auxiliary heater can achieve notable energy savings. Bertram et al. [12] investigated the performance of a solar-assisted heat pump system with a ground heat exchanger by using TRNSYS, and their results showed that directly using solar energy can achieve the best efficiency improvement. Qu et al. [13] investigated the energy efficiency of a solar heat pump heating system with dual-tank latent heat storage achieved using phase-change materials (PCMs), and they concluded that PCMs can improve the energy efficiency of the proposed system. Lerch et al. [14] comparatively analyzed the performance of different combinations of solar energy and heat pump systems, showing that the solar collectors combined with a heat pump in parallel have a higher efficiency than conventional air source heat pumps. Liu et al. [15] compared the performance of a solar-air composite heat source heat pump system in two different modes at two ambient temperatures, showing that the system has a higher heat capacity and coefficient of performance (COP) in solar-air dual heat source mode.

However, many factors can affect the performance of solar combisystems, such as climatic conditions. In this study, the effect of climate was considered in order to determine suitable systems for different climatic conditions, accounting for both cost and efficiency. The literature includes many experiments and simulations of solar combisystems and discussions of the effect of climatic conditions.

Asaee et al. [3] simulated the effect of a solar-assisted heat pump (SAHP) system in Canada; their analysis revealed that the SAHP system is strongly affected by climatic conditions and the heat source of the auxiliary heater, and that energy consumption and greenhouse gas emissions can be reduced by approximately 20% with the SAHP system. Poppi et al. [16] numerically simulated the thermal performance and costs of solar thermal and air source heat pump combisystems in two cities (Zurich and Carcassonne), showing that the cost-effectiveness and thermal performance of the systems were affected by their distinct climatic conditions. Jradi et al. [17] developed a combined PV–air source heat pump system to supply electricity and heating in Denmark, and they showed that this proposed system can improve the efficiency of conventional systems and increase the reliability and stability of energy supply. This system can not only enhance efficiency but also reduce the emission of greenhouse gases in Denmark. Using a numerical model, Rad et al. [18] analyzed hybrid solar thermal and ground-source heat pump systems in six different cities in Canada to determine the effect of climatic conditions. They found that such systems were most viable in Vancouver, which has the mildest climate of the considered cities. Awani et al. [19] performed both a numerical analysis and an experiment on a heat pump system assisted by solar and geothermal energy in Tunisia, showing that Tunisia has thermal potential through its geothermal energy supply and that the COP of this system can reach 5.5. The system also represents considerable energy savings over traditional heating systems. Tzivanidis et al. [20] analyzed three different water heating systems in Athens and found that the air source heat pump system had the lowest cost, but the system with a solar driven heat pump had a much higher efficiency and lower energy consumption, making it more attractive than other systems. Zhu et al. [21] numerically analyzed the feasibility, economy, energy savings, and environmental protection features of solar water heat pump systems in three different cities with distinct climatic conditions (Harbin, Beijing, and Shanghai). Their results revealed that the system has superior applicability in colder regions. Chow et al. [22] found that the average efficiency of a direct-expansion SAHP system is higher than that of other conventional heat pump systems, and that this system has potential applications in Hong Kong.

Moreover, some researchers have employed the Taguchi method to optimize the heating performance of heat pumps. The most important feature of the Taguchi method is the use of an orthogonal-array experimental design with a single analysis of variance. The signal-to-noise (S/N) ratio is used to assess quality characteristics deviating from the desired value.

Esen et al. [23] used the Taguchi method to optimize a vertical ground-coupled heat pump system with 3.75 as the optimal COP value. Sivasakthivel et al. [24] applied the Taguchi method to analyze a ground-source heat pump system for space cooling and heating [17], concluding that parameters such as the inlet and outlet temperatures of the condenser and evaporator can be optimized through the Taguchi method. The maximum COP was determined to be 4.25 for the heating-only mode and 3.32 for the cooling-only mode. Murugesan et al. [25] used the Taguchi method to optimize a solar-assisted ground-source heat pump system, and found the maximum COP value to be 3.86. Li et al. [25] investigated the system performance of a direct-expansion solar-assisted heat pump water heater. Kumar et al. [26] used artificial neural network (ANN) integrated with genetic algorithm (GA) to predict the performance of direct expansion solar assisted heat pump. Dott et al. [27] evaluated several configurations of solar collectors and heat pumps regarding the direct or indirect uses of solar irradiation. Poppi et al. [28] numerically investigated the effects of climate, load, and main component size on electricity use.

Single- and dual-tank solar combisystems prevail currently because of their straightforward hydraulic systems, easy maintenance, well-developed technology, and highly reliable performance. However, weather factors such as solar radiation, ambient temperature, and relative humidity can influence the heating performance of the solar collector and heat pump. When the solar collector and heat pump are engaged in combination, the operating parameters of the combisystem are associated with the overall performance of a solar domestic hot water (SDHW) system. Prioritizing the operating parameters of solar collectors and heat pumps in solar combisystem designs has generally been empirical or speculative, leading to design redundancy and performance overestimation. To obtain a significant reduction in work input or increase in heating performance, both the water tank volume and the flow rate must be optimized. For this purpose, the present study proposes employing the Taguchi method. Three influencing factors for single-tank systems and four factors for dual-tank combisystems were considered for the analysis.

The Taguchi method is feasible for optimizing heat pump performance by determining the COP value, but not for analyzing the performance of solar collectors by determining the solar fraction (SF) ratio [29]. The SF is defined as the fraction of solar input to the tank to the total input to the tank. However, it is subject to distorted evaluations of the S/N ratio, because a larger solar collector area is associated with a higher SF; the alleged optimal results would simply involve the largest solar collector area for the solar loop and the smallest water tank volume for the heat pump. To avoid such inappropriate evaluations, it is necessary to modify the S/N ratio assessment and determine the true optimal operating parameters in terms of both climatic conditions and hydraulic layout.

2. Simulation model and description

2.1. Numerical software

In this study, the commercial software TRNSYS 17 [26] was employed to analyze the effects of hydraulic layouts on domestic hot water (DHW) systems and the feasibility of various solar combisystems in multiple metropolitan areas with distinct climatic conditions. The performance of a solar combisystem with a heat pump is sensitive to the degree of correlation between the ambient temperature and solar irradiation. The simulated results were validated with the experimental results of a system physically implemented in a previous study [27].

The parameter settings of the solar collector model were adjusted to improve the simulation accuracy. The software enables modeling the hydraulic layout of the solar combisystem and simulating its heating performance with various water draw schedules and climatic conditions. Many of the models in the standard TRNSYS library were leveraged, including Type 1 (quadratic efficiency collector), Type 3 (pump), Type 2b (controller), and Type 15 (weather data reading and processing). In the demonstration system [27], civil water was directly pumped into the solar collectors and heated via solar thermal energy. The hot water heated by the solar collector was delivered and stored in the storage tank. Similarly, the hot water heated by the heat pump would be delivered and stored in the storage tank. There is no heat exchanger unit in the solar loop. Type 4a was appropriate to simulate the real situation of water storage tank. The climate database TMY2 (Typical Meteorological Years) comprises 10 years of meteorological data and provides statistical climatic conditions for TRNSYS simulation. Two individual hydraulic layouts were considered in this study, namely a single-tank solar combisystem and a dual-tank solar combisystem.

The heat pump used in the TRNSYS model was a Type 938 air-to-water heat pump. An external file determined the energy characteristics of the heat pump. The profile consisted of two inlet water temperatures (9 °C and 15 °C), two air temperatures (7 °C and 20 °C), and two air-relative humidity levels (58% and 80%); the profile generated a table that determined the power consumption, heating capacity, and cooling capacity levels for all combinations of these values. Other operational points were determined through linear interpolation from this data. The heat pump model read the input load and source temperatures and then used the external file to determine the power consumption and the energy transfer. In this system, the rated heating capacity of the heat pump was 7 kW, and its power was 1.7 kW.

The simulation software was programmed to ensure that all systems delivered the same water temperature and had the same water draw schedule for all configurations. In TRNSYS, each tank was divided into 10 nodes of equal size to simulate stratification. An overall uniform loss coefficient of 0.833 W/m^2K was applied to each tank; the simulated water was given a specific heat of 4.19 kJ/kgK to simulate real water.

2.2. Single-tank solar combisystem

Fig. 1 shows the simulated model and layout of the single-tank solar combisystem, which involves a solar water heating system combined with a heat pump in parallel. The components and detailed parameters are listed in Table 1. In addition, two separate loops required control. The solar loop, a hydraulic loop between the solar collector and the domestic water (DW) tank, was controlled in the manner of a traditional SDHW system; when the outlet temperature of the collector was 7 °C higher than the temperature of the water at the bottom of the tank, the pump in the solar loop was turned on. The system continued to operate until this temperature difference fell below 3 °C. The heat pump loop (a hydraulic loop between the heat pump and the DW tank), which supplied energy to the DW tank, was turned on when the water in the middle of the DW tank fell below 50 °C, and it remained active until the water had been heated to the set point temperature (55 °C). In this system, the rated heating capacity of the heat pump was set to 7 kW and its rated input power to 1.7 kW. This arrangement ensured that the DW tank was constantly charged and able to supply various water draws.

The volume of the thermal storage tank, flow rate of the solar collector, and flow rate of the heat pump are essential to determining the overall heating performance of the single-tank solar combisystem with the Taguchi method. This study discusses the effect of these three parameters. The weather component of the numerical model could receive input related to different climates, enabling us to analyze and optimize the solar combisystem in different climatic conditions. The solar collector area was fixed at 5 m^2, and the intercept efficiency, efficiency slope, and efficiency curvature were 0.6, 6.8 and 0.4, respectively. The main loop of this combisystem involved water delivered to the solar collector via a pump (controlled by the controller), heated via the solar collector, and then transferred to a thermal storage tank. If the water temperature was below the demand temperature, the heat pump would turn on and further heat the water. The system simulated the 40 °C hot water consumption of a typical four-person family with 1-h water draws at a rate of 300 L/hr per person from 09:00 to 10:00 and 21:00 to 22:00, and the operating time of the heat pump was set from 08:00 to 10:00 and 20:00 to 22:00 for every simulated day. The time schedule of hot water supply is from 9:00 to 10:00 in the morning and from 21:00 to 22:00 in the evening. This water draw profile may not have been realistic, but it sufficed for drawing comparisons.

2.3. Dual-tank solar combisystem

Fig. 2 shows the layout and simulation model of the dual-tank solar combisystem. The solar loop was controlled in the same manner as in a traditional SDHW system without an auxiliary heating unit. When the outlet temperature of the collector was 7 °C higher than the temperature of the water at the bottom of the tank, the pump in the solar loop was turned on. The collected energy was stored in the storage tank. In the second loop, the heat pump was used to provide energy to the smaller DW tank. A pump with a power of 60 kJ/hr moved water from the storage tank to the DW tank. Cold civil water was fed into the storage tank, and the outflow of the storage tank was pumped into the DW tank.

A dual-tank solar combisystem can reduce the competition between two heating sources during the day, and it can also reduce the load on the heat pump during the night because of the relatively small DW tank. However, the second tank in a dual-tank solar combisystem increases incremental costs and complicates heat loss issues. Therefore, the four parameters examined in this study are the volumes of two thermal storage tanks, flow rate of the solar collector, and flow rate of heat pump. The control factors were assumed to be independent of each other and each factor had three levels. The weather component could simulate different climates and optimize the heating performance of the system under different climatic conditions. The parameter settings of the solar collector and heat pump were the same as the single-tank solar combisystem. In the main loop of this combisystem, water was delivered to the solar collector through the pump, heated via the solar collector, transferred to the first tank, and pumped to the second tank if the water of the second tank was used. If the water temperature was lower than required, the heat pump would turn on and further heat the water of the second tank to satisfy the thermal demand. The time schedule and flow rate of water

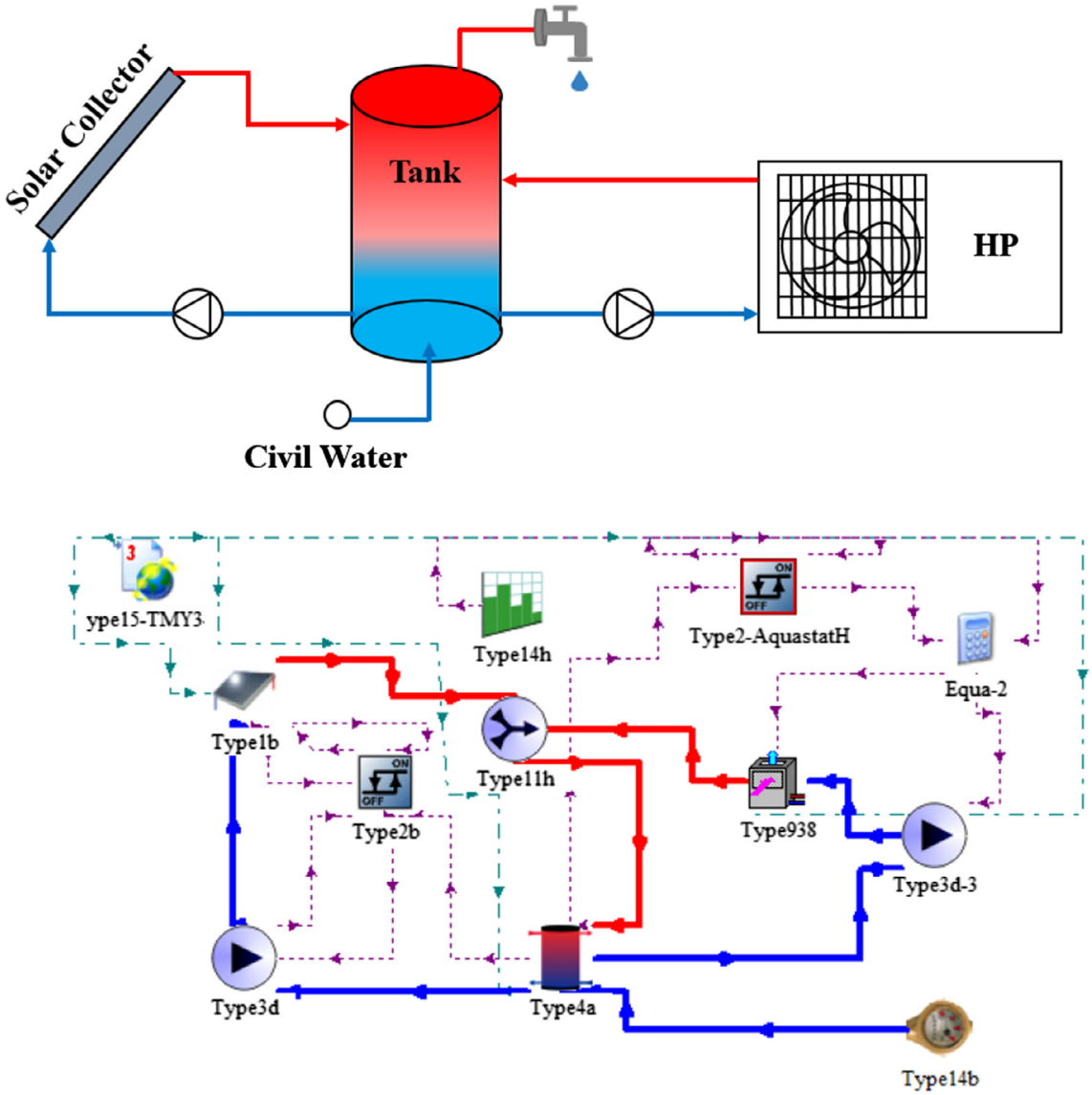

Fig. 1. Schematics and simulation model of solar collector and heat pump in a single-tank combisystem.

Table 1
Single-tank control factors and parameter levels.

Label	Parameters	Level		
		L1	L2	L3
A	Volume of tank (L)	300	400	500
B	Flow rate of HP (kg/h)	200	300	400
C	Flow rate of SC (kg/h)	100	200	300

consumption and the operating time of the heat pump were the same as in the single-tank system.

3. Methodology

Taguchi optimization is an experimental technique that uses a standard orthogonal array of experiments in matrix form, which gives an optimal number of experimental trial runs with optimum control parameter settings. This technique enables determining the best level of each parameter. In this method, the number of control parameters and levels must be identified for the system under initial consideration. Based on the number of control parameters and levels, the appropriate orthogonal array must be selected to specify the optimal number of trial runs to be performed. Eventually, the results obtained for each trial run are analyzed using the S/N ratio, analysis of variance (ANOVA), and a response table.

The S/N ratio is used to assess the quality characteristics approaching the ideal value. Three types of performance characteristics can be used for analyzing the S/N ratio: the lower the best, the higher the better, and the nominal the best. ANOVA is to indicate which design parameters significantly affect the output parameters. The results of both analyses provide information on the influential parameters and their levels.

Because the present research was concerned with the optimal heating performance of the system, the higher-the-better criterion was selected. Thus, the initial cost of the solar combisystem could be reduced. In general, the COP is a receivable indicator to assess the operational optimization of a heat pump system, whereas the SF value is used to understand the contribution of solar thermal energy in SDHW systems. Because of the aforementioned bias issues, a new indicator (σ) is proposed to appraise the overall performance of solar combisystems,

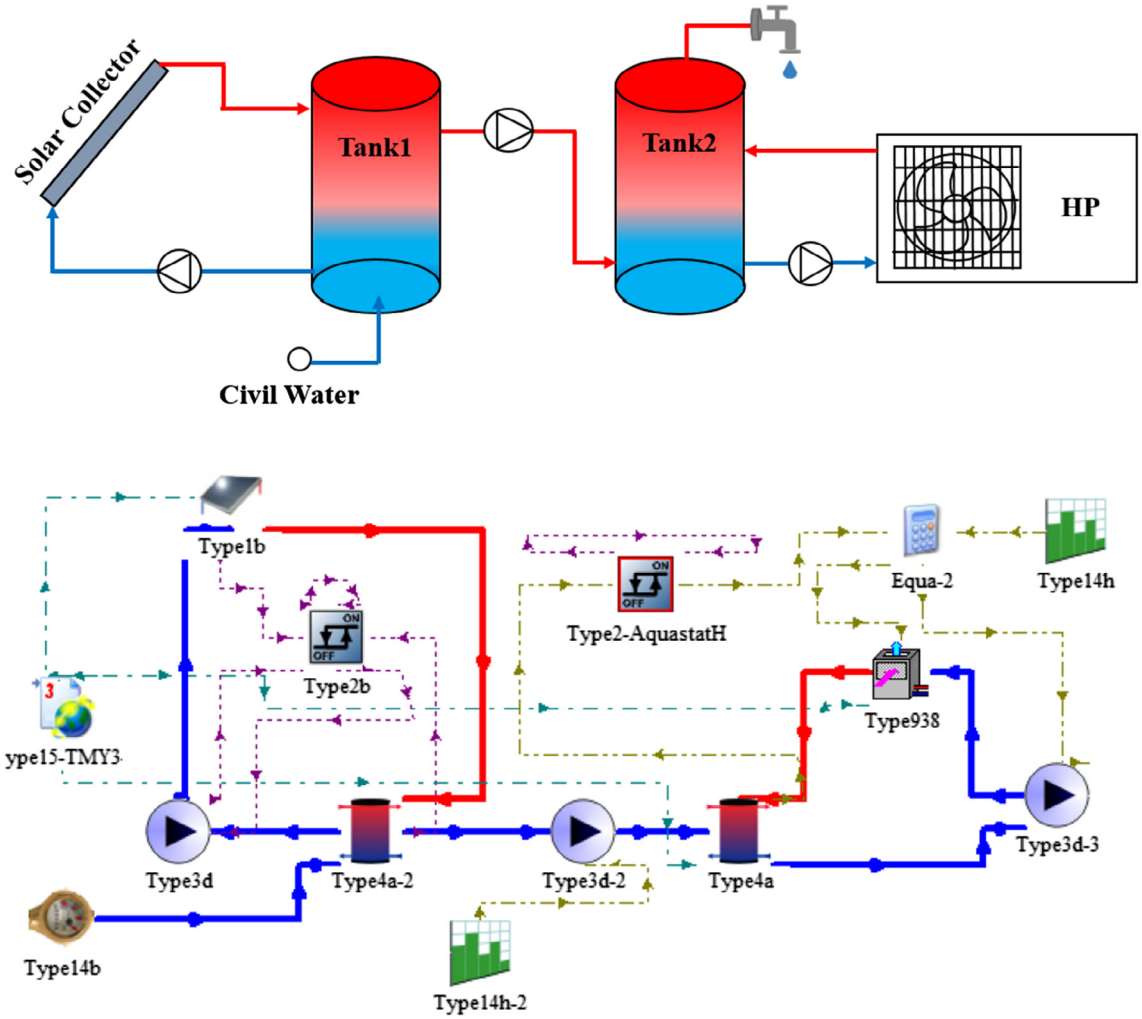

Fig. 2. Schematics and simulation model of solar collector and heat pump in a dual-tank combisystem.

$$\sigma = [\overline{(Q_{hp}/W_{hp})} + \overline{(Q_{solar}/W_{solar})}], \quad (1)$$

where σ is an indicator of the system's overall performance, Q_{hp} is the heating capacity of the heat pump, Q_{solar} is solar-collected thermal energy, and W_{hp} and W_{solar} are the electric consumption of the heat pump system and SDHW system, respectively. Because of the value difference of the two ratios, namely (Q_{hp}/W_{hp}) and (Q_{solar}/W_{solar}), they are normalized before being converted into S/N ratios. The normalization process involves dividing the individual $(Q_{hp}/W_{hp})_i$ by the maximum ratio of the control group $(Q_{hp}/W_{hp})_{max}$, and dividing the individual $(Q_{solar}/W_{solar})_i$ by the maximum ratio of the control group $(Q_{solar}/W_{solar})_{max}$. Accordingly, the values of the two normalized indicators, $\overline{(Q_{hp}/W_{hp})}$ and $\overline{(Q_{solar}/W_{solar})}$, span from 0 to 1.

To determine the heating performance of the single-tank solar combisystem, the following three operating parameters were considered control factors: (A) tank volume, (B) flow rate of the solar collector, and (C) flow rate of the heat pump. For the dual-tank system, the four control factors were (A) first tank volume, (B) flow rate of the solar collector, (C) flow rate of the heat pump, and (D) second tank volume. Tables 1 and 2 show the control factors and their levels for the dual-tank and single-tank solar combisystems. Because the control factors (three control factors in the single-tank system and four control factors in the dual-tank system) were assumed to be independent of each other, and because each factor had three levels, an L_9 orthogonal array was used and the experimental number was reduced to nine experiments, as shown in Table 3 for the single-tank system and Table 4 for the dual-tank system. The S/N ratio for the higher-the-better characteristics is defined as follows:

Table 2
Dual-tank control factors and parameter levels.

Label	Parameters	Level		
		L1	L2	L3
A	Volume of tank (L)	400	500	600
B	Flow rate of HP (kg/h)	200	300	400
C	Flow rate of SC (kg/h)	100	200	300
D	Volume of second tank (L)	200	250	300

$$\frac{S}{N} = -10\log\left(\frac{1}{n}\sum_{i=1}^{n}\frac{1}{Y_i^2}\right), \quad (2)$$

where n is the number of tests and y_i is the value of the σ indicator.

To determine the effect of different climatic conditions, the solar combisystems were investigated and Taguchi-optimized for five simulated cities representing distinct climates: Tainan (tropical monsoon), Lisbon (Mediterranean), Hong Kong (subtropical monsoon), Osaka (humid subtropical), and Madrid (continental).

Table 3
Orthogonal array for single-tank solar combisystem.

Numerical No.	A	B	C
1	300	200	100
2	300	300	200
3	300	400	300
4	400	200	200
5	400	300	300
6	400	400	100
7	500	200	300
8	500	300	100
9	500	400	200

Table 4
Orthogonal array for dual-tank solar combisystem.

Numerical No.	A	B	C	D
1	400	200	100	200
2	400	300	200	250
3	400	400	300	300
4	500	200	200	300
5	500	300	300	200
6	500	400	100	250
7	600	200	300	250
8	600	300	100	300
9	600	400	200	200

The incremental capital costs of the solar combisystems were also considered, and realistic payback periods were calculated to determine their economic feasibility.

4. Results and discussion

The five cities have distinct climatic conditions during the four seasons, which were represented by ambient temperature (Fig. 3) and relative humidity (Fig. 4) data from the TMY2 database, as well as the incident solar radiation (Fig. 5). The optimal tilt angle of the solar panel is related to the latitude of the deployed location; therefore, the incident solar radiation represents the real solar radiation reaching the solar panel, subtracting for the amount of solar reflection and absorption induced by the ambient conditions.

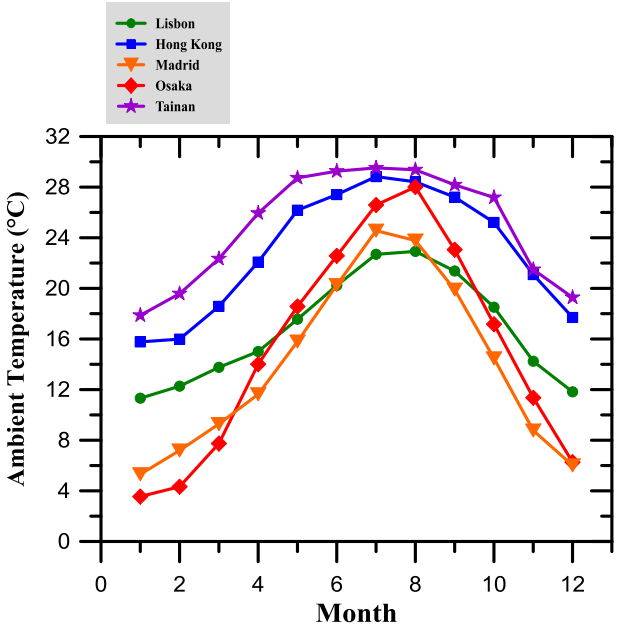

Fig. 3. Annual ambient temperatures of five cities.

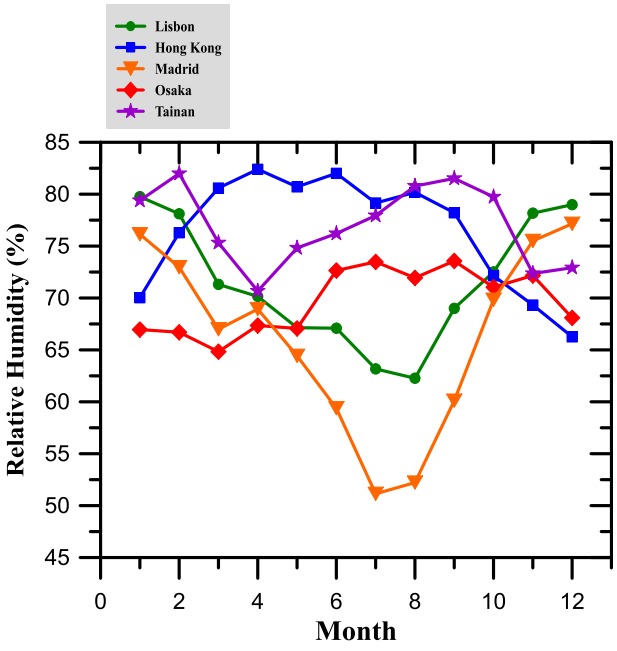

Fig. 4. Annual relative humidity of five cities.

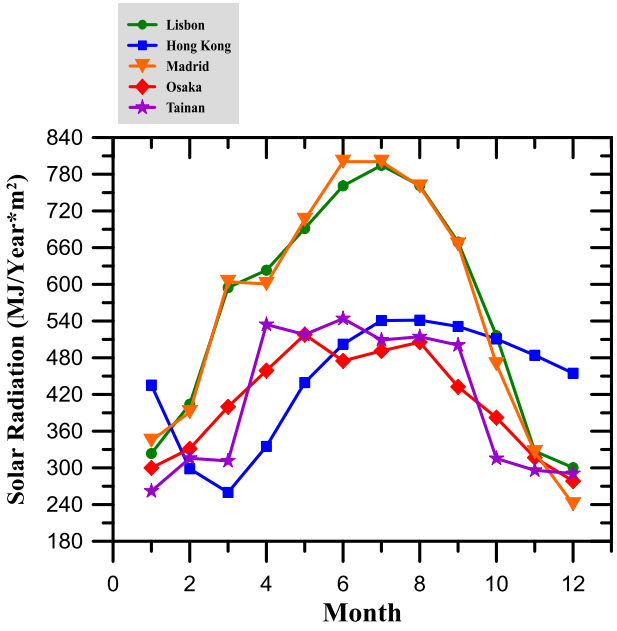

Fig. 5. Annual solar radiation of five cities.

Tainan (22°59′N, 120°11′E) has a tropical monsoon climate, characterized by high relative humidity and temperature. Its ambient temperature is higher than those of Osaka, Madrid, and Lisbon, and it also has a rainy season from April to September and a dry season from October to March.

Madrid (40°45′N, 3°55′W) has a continental climate with a hot summer and cold winter. Its rainy season is concentrated during the autumn and spring; it seldom rains in summer and it has a dry climate, with lower relative humidity and higher solar radiation than the summer days of Tainan, Hong Kong, and Osaka (Fig. 4).

Osaka (34°78′N, 135°45′E) has a humid subtropical climate with four distinct seasons. Winter is the coldest and driest season because of decreased rainfall, and the coldest month is January.

Table 5
The climate features of five cities.

City	Location	Climatology	Climate Feature
Tainan	22°59′N, 120°11′E	Tropical monsoon climate	It is high relative humidity and temperature, and the rainy season is from April to September and a dry season from October to March
Madrid	40°45′N, 3°55′W	Continental climate	The rainy season is concentrated during the autumn and spring; it seldom rains in summer and it has a dry climate, with lower relative humidity and higher solar radiation
Osaka	34°78′N, 135°45′E	Humid subtropical climate	Winter is the coldest and driest season, and the coldest month is January. The rainiest period is during summer. After summer, the rainfall decreases in fall along with the temperature
Hong Kong	22°3′N, 114°17′E	Humid subtropical climate	Summer is hot and humid because of occasional showers and thunderstorms. Winters are mild and sunny, and spring is sunny, dry, and temperate
Lisbon	38°72′N, 9°15′W	Mediterranean climate	Mediterranean climate has mild and rainy winters and hot and dry summers. The coldest month is January

Therefore, the ambient temperature is low in winter and the average ambient temperature is lower than those in Tainan, Hong Kong, and Lisbon (Fig. 3). The rainiest period is during summer, which is Osaka's wettest season with hot and humid days. After summer, the rainfall decreases in fall along with the temperature.

In Hong Kong (22°3′N, 114°17′E), summer is hot and humid because of occasional showers and thunderstorms and warm air coming from the southwest. Winters, by contrast, are mild and sunny and spring is sunny, dry, and temperate. Hong Kong has a high sunshine period, receiving approximately 1948 h of year-round sunshine. Therefore, the ambient temperature remains high in winter, and the average temperature is higher than those in Osaka, Lisbon, and Madrid.

Lisbon (38°72′N, 9°15′W) has a Mediterranean climate with mild and rainy winters and hot and dry summers. The coldest month is January. Lisbon's solar radiation is high, given its high sunshine hours (nearly 2800 per year); the average daily sunshine duration in December is approximately 4.6 h, and that in July is nearly 11.4 h. Therefore, Lisbon has higher incident solar radiation than Osaka, Hong Kong, and Tainan (Fig. 5).

Madrid and Lisbon have high solar radiation from March to October, but low solar radiation from November to February because of their rainy seasons. Tainan and Osaka have considerable solar radiation from April to September but weak solar radiation from October to March. The period from February to May is Hong Kong's rainy season, leading to low solar radiation, but it has good solar radiation from June to January. Notably, cities near the equator or Tropic of Cancer are humid due to strong convection, with the moisture and clouds leading to strong solar reflection and absorption. Table 5 lists the climatology and climate features of these five cities for comparison.

Table 6
Taguchi response table for the single-tank system performance in five cities.

Tainan			
	L1	L2	L3
A	5.651034	5.676988	5.759140
B	5.931043	5.520224	5.635895
C	5.679223	5.742446	5.665494
Madrid			
	L1	L2	L3
A	5.478906	5.614106	5.667136
B	5.792535	5.376988	5.590625
C	5.473478	5.567943	5.718727
Osaka			
	L1	L2	L3
A	5.640995	5.635711	5.694227
B	5.877107	5.362140	5.731685
C	5.676508	5.705266	5.589158
Hong Kong			
	L1	L2	L3
A	5.631786	5.737893	5.767151
B	5.898728	5.525773	5.712330
C	5.735995	5.743469	5.657367
Lisbon			
	L1	L2	L3
A	5.472966	5.502678	5.616612
B	5.712297	5.342065	5.537895
C	5.368797	5.534021	5.689438

4.1. S/N ratio analysis

According to the Taguchi method, the optimal parameters for the solar combisystems can be found by examining their S/N ratios. Therefore, the mean S/N ratios for each level of the control parameters were calculated, and they are summarized in the S/N response tables for the best overall performance of the single-tank (Table 6) and dual-tank (Table 7) systems in each of the five cities.

Table 7
Taguchi response table for the dual-tank system performance in five cities.

Tainan			
	L1	L2	L3
A	5.824663	5.838587	5.811549
B	5.827556	5.878257	5.768986
C	5.673079	5.892212	5.909509
D	5.869046	5.830054	5.775699
Madrid			
	L1	L2	L3
A	5.697954	5.796282	5.829912
B	5.948537	5.766162	5.709449
C	5.630912	5.858856	5.834379
D	5.858659	5.772012	5.693478
Osaka			
	L1	L2	L3
A	5.694941	5.786526	5.811775
B	5.834192	5.764863	5.694187
C	5.545639	5.880835	5.866768
D	5.827306	5.767128	5.698808
Hong Kong			
	L1	L2	L3
A	5.801172	5.842883	5.847347
B	5.866133	5.861980	5.763289
C	5.675413	5.903610	5.912378
D	5.886375	5.837067	5.767960
Lisbon			
	L1	L2	L3
A	5.622271	5.550087	5.738588
B	5.745817	5.558177	5.606952
C	5.504208	5.692476	5.714262
D	5.597613	5.685578	5.627755

The S/N values given in Table 6 are also depicted in the form of illustration in Fig. 6 for better understanding the influencing parameters. The optimal parameters for the single-tank system in Tainan, Madrid, Osaka, Hong Kong, and Lisbon were determined to be (A3 B1 C2), (A3 B1 C3), (A3 B1 C2), (A3 B1 C2) and (A3 B1 C3), respectively. For all locations, the optimal value of factor A (tank volume) was A3, because large tank volumes store more solar radiation, and the optimal value of factor B (heat pump flow rate) was B1, because if it were much higher, the competition between the solar collector and heat pump would increase and the efficiency would decrease; therefore, the lower value is best. The optimal value of factor C (solar collector flow rate), however, varied for some of the cities. Madrid and Lisbon receive more solar radiation than the other locations (Fig. 4), resulting in more collected solar thermal energy; therefore, the corresponding optimal value was C3. For the other cities, the optimal value was C2.

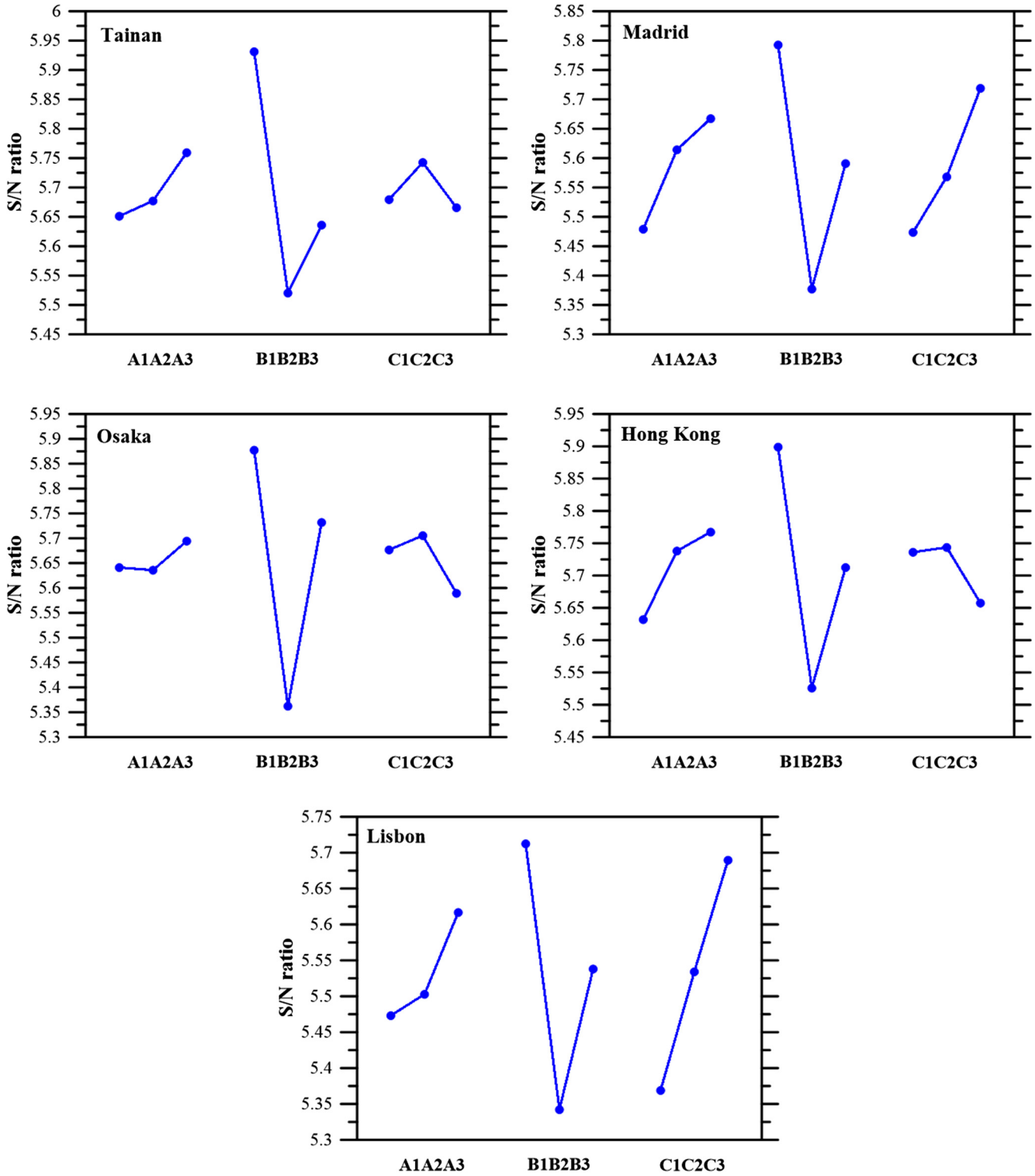

Fig. 6. Effect of control parameters on the performance of the single-tank system in five cities.

For the dual-tank system, factor D (volume of the second tank) was also included. The S/N values given in Table 7 are also depicted in the form of illustration in Fig. 7 for better understanding the influencing parameters. The optimal set of control parameters are presented in Fig. 7: Tainan (A2 B2 C3 D1), Madrid (A3 B1 C2 D1), Osaka (A3 B1 C2 D1), Hong Kong (A3 B1 C3 D1), and Lisbon (A3 B1 C3 D2). These values differed from their single-tank counterparts. The optimal value for factor A (A2) in Tainan was significant because of the lower solar radiation and higher ambient temperature in this region (Figs. 3 and 4). Given this situation, more work is required for the solar collector to extract heat from solar radiation and a larger tank volume would consume more electricity. Owing to the fact of low solar radiation and high ambient temperature in Tainan, the heating performance of heat pump in DHW system is presumably predominant. The optimal flow rate of the heat pump in Tainan is higher than those of the other

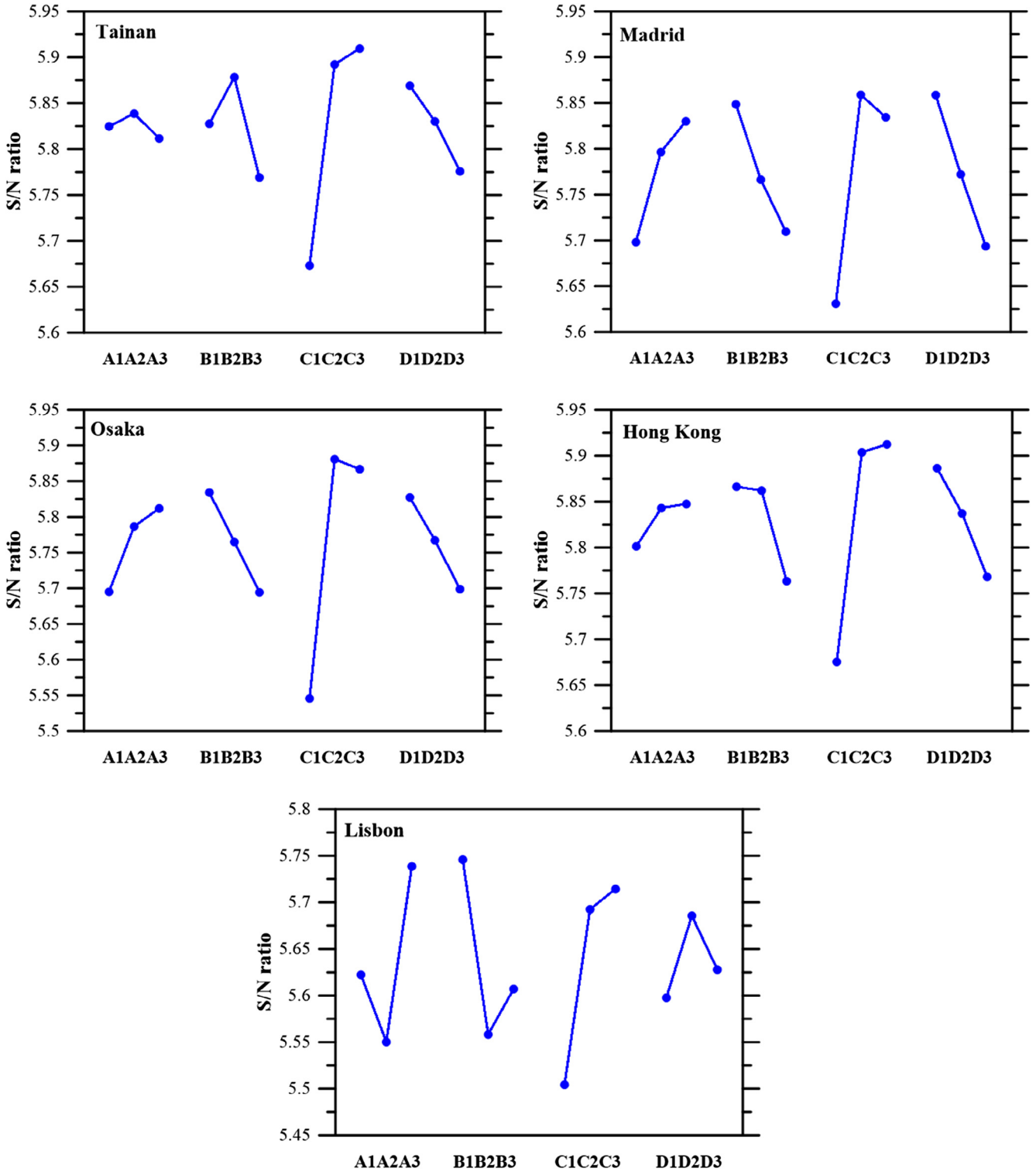

Fig. 7. Effect of control parameters on the dual-tank system performance in five cities.

locations due to easily extracting thermal energy from the ambient. Hong Kong has similar climatic conditions but more solar radiation during the winter, making its optimal value A3.

The optimal value of factor C in Madrid and Osaka differed from the other locations because a higher flow rate of the solar collector would cause short residence time and low outlet water temperature of solar collector. The ambient temperatures of these two locations (Madrid and Osaka) are lower than those of the others (Fig. 3), making heat loss from the pipes a substantial concern and resulting in a different optimal value for factor C.

Regarding factor D, Lisbon's high solar radiation and the larger volume of the second tank result in more thermal energy being collected via solar panels. However, increasing the water tank volume would impact the COP of the heat pump from heating the extra water; therefore, the optimal value was D2. However, although Madrid matches Lisbon in terms of solar radiation, its optimal value was D3 because Madrid's ambient temperature is lower, making heat loss more of a concern. A larger tank would cause greater heat loss and decrease the overall efficiency. This thus explains factor D having different optimal values for these two cities.

4.2. Contribution of each control factor on the single-tank system

From the ANOVA results shown in Fig. 8, the sum of squares (SS) and the contribution were calculated to examine the effect of each control parameter on the performance of the single-tank system for each of the five cities. According to the results, the respective contributions of the parameters A, B, and C were 7%, 90%, and 3% in Tainan; 14%, 64%, and 22% in Madrid; 1%, 94%, and 5% in Osaka; 12%, 83%, and 5% in Hong Kong; and 9%, 52%, and 39% in Lisbon. This reveals the flow rate of the heat pump to be the most significant parameter affecting the single-tank system performance in all locations.

According to Fig. 4, the solar radiation of Tainan is low. Therefore, the contribution of factor B was high and that of factor C was low. This would reduce the competition between the solar collector and heat pump, rendering the contribution of factor A low. However, despite the contribution of factor B being the highest of all factors in Madrid and Lisbon, it was not as high there as in Tainan, Hong Kong, and Osaka. The high solar radiation of Madrid and Lisbon can be attributed to the increase in the contribution of factor C. The contribution of factor B was also decreased because of the lower relative humidity in Madrid and Lisbon; the heat pump performs better when the relative humidity is higher. Moreover, this heightens the competition between the solar collector and heat pump, increasing the contribution of factor A.

The contribution rate of factor B was higher in Osaka than the other locations due to its lower solar radiation and ambient temperature (Figs. 3 and 4); because of the extremely high contribution of factor B, the competition between factors C and B was determined to be low, reducing the contribution of factor A.

Although Hong Kong's overall solar radiation is not as high as that of Madrid and Lisbon, it is high during winter (Fig. 4), and heat

Tainan

Factor	SS	Contribution
A	0.01911	6.40244%
B	0.26926	90.21040%
C	0.01011	3.38716%
Total	0.29848	100%

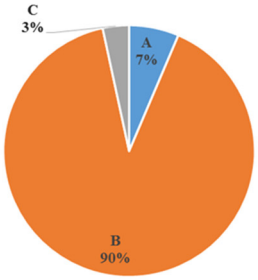

Madrid

Factor	SS	Contribution
A	0.05652	13.87266%
B	0.25909	63.59285%
C	0.09181	22.53449%
Total	0.40742	100%

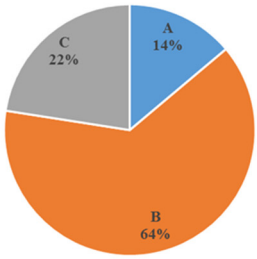

Osaka

Factor	SS	Contribution
A	0.00629	1.39428%
B	0.4229	93.74238%
C	0.02194	4.86334%
Total	0.45113	100%

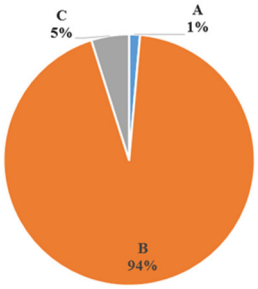

Hong Kong

Factor	SS	Contribution
A	0.03044	12.04447%
B	0.20864	82.55450%
C	0.01365	5.40102%
Total	0.25273	100%

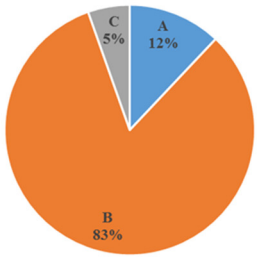

Lisbon

Factor	SS	Contribution
A	0.0345	8.74303%
B	0.20584	52.16422%
C	0.15426	39.09275%
Total	0.3946	100%

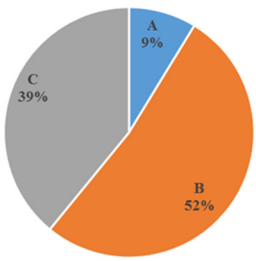

Fig. 8. Contribution of each parameter for a single-tank system in five cities.

pumps are operated the most during winter because of the low ambient temperature. Therefore, the contribution rate of factor B was not as high as in Tainan and Osaka, increasing the competition between factors C and B and raising the contribution rate of factor A. The total solar radiation is similar to that of Tainan and Osaka, and the contribution rate of factor C was thus not high.

4.3. Contribution of each control factor on the dual-tank system

As with the single-tank system, the sum of squares and the contribution were calculated to examine the effect of each control parameter on the performance of the dual-tank system in the five locations. According to the results (Fig. 9), the contributions of factors A, B, C, and D were, respectively, 1%, 13%, 76%, and 8% in Tainan; 3%, 13%, 70%, and 14% in Madrid; 8%, 10%, 74%, and 10% in Osaka; 3%, 13%, 70%, and 14% in Hong Kong; and 27%, 28%, 39%, and 6% in Lisbon. This reveals the flow rate of the solar collector (C) to be the most substantial control parameter in all locations. This result differs from the single-tank system because the solar and heat pump loops are separated into two thermal storage tanks, rendering the competition between the solar collector and heat pump nonexistent.

The contribution of factor A relates to the solar radiation: the larger the tank volume is, the more solar energy can be stored when the solar radiation is high (e.g., in Madrid and Lisbon). Factor B could also be affected by solar radiation; its contribution rate increased with high solar radiation. The water draw was fixed at a rate of 300 L/hr. At a low heat pump flow rate, the consumption rate of hot water in the second tank is slow, and the water delivered from the first tank to the second is correspondingly low. This leads to a low reduction of the water temperature in the first tank, decreasing the efficiency of solar thermal collection. However, at a

Tainan

Factor	SS	Contribution
A	0.0011	0.80616%
B	0.01794	13.14767%
C	0.10422	76.37963%
D	0.01319	9.66654%
Total	0.13645	100%

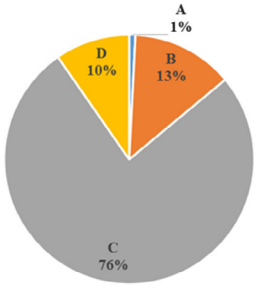

Madrid

Factor	SS	Contribution
A	0.02821	14.65607%
B	0.02935	15.24834%
C	0.09396	48.81546%
D	0.04096	21.28013%
Total	0.19248	100%

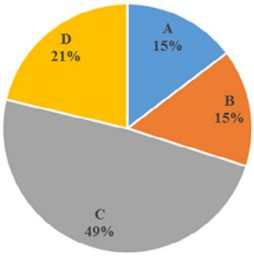

Osaka

Factor	SS	Contribution
A	0.02268	7.75226%
B	0.0294	10.04922%
C	0.21568	73.72163%
D	0.0248	8.47689%
Total	0.29256	100%

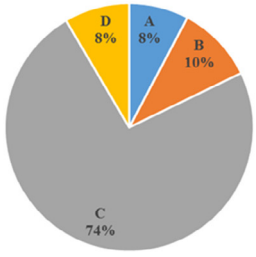

Hong Kong

Factor	SS	Contribution
A	0.00389	2.53008%
B	0.02033	13.22276%
C	0.1083	70.43902%
D	0.02123	13.80813%
Total	0.15375	100%

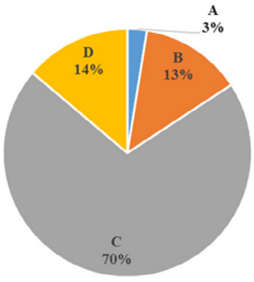

Lisbon

Factor	SS	Contribution
A	0.05427	26.71162%
B	0.05687	27.99134%
C	0.08004	39.39558%
D	0.01199	5.90146%
Total	0.20317	100%

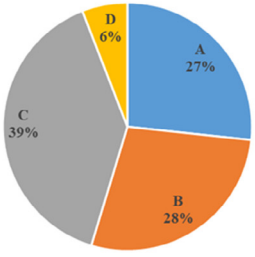

Fig. 9. Contribution of each dual-tank system parameter in five cities.

Table 8
Equipment cost in five cities.

Location	GNP (USD)	Equipment cost (USD)				
		Gas heater	Electrical heater	SDHW	Combi-Single	Combi-Dual
Tainan	23,229	750	1000	1990	3550	4010
Madrid	28,520	920.83	1227.78	2443.27	4358.60	4923.38
Osaka	36,680	1184.30	1579.06	3142.33	5605.67	6332.03
Hong Kong	41,000	1323.78	1765.04	3512.42	6265.87	7077.79
Lisbon	20,530	662.86	883.81	1758.78	3137.52	3544.07

high heat pump flow rate, the water delivered from the first tank to the second increases. The water temperature in the first tank is reduced because of the supply of cold water from the mains, leading to an improvement in the solar panel efficiency.

Although the solar radiation of Madrid and Lisbon are comparably high, the contribution rate of factor B in Madrid was not as high because of its lower ambient temperature. Where ambient temperatures are low, the contribution rate of factor B was correspondingly low; this holds for Osaka as well as Madrid, although Madrid's solar radiation is much higher than Osaka's. In cold ambient temperatures, the efficiency of the heat pump drops, reducing the flow rate of the heat pump.

Regarding factor C, low solar radiation results in the low flow rate for the solar collector, reducing the collected thermal energy. A high flow rate of the solar collector does not effectively harvest extra thermal energy, but the power consumption of the water pump would increase. Accordingly, in regions with low solar radiation (Hong Kong, Tainan, and Osaka), the importance factor C becomes evident.

The contribution rate of factor D was also affected by the solar radiation. The volume of the second tank is associated with the probability and capacity of the first tank to supply water to the second tank, affecting the water temperature of the first tank and further influencing the thermal efficiency of the solar collector and the operating time of the heat pump. Therefore, when solar radiation is higher, the influence of factor D could increase. The solar radiation in Lisbon is similar to that in Madrid, but factor D was diminished in Madrid because its low ambient temperatures exacerbate the issue of heat loss. By contrast, the high ambient temperatures in Lisbon render the impact of factor D relatively high.

4.4. Comparing the payback periods of DHW systems

This study not only considered the technical aspects of solar combisystems, but also estimated realistic payback periods and gauged their economic feasibility.

The dual-tank combisystem has a higher initial equipment cost than the single-tank system. The equipment costs for Madrid, Osaka, Hong Kong and Lisbon were calculated by comparing the GNP with Taiwan (Table 8). In Taiwan, the retail price of a heat pump with a heating capacity of 7 kW was determined to be approximately US$1500, an additional DW tank was calculated to be US$460, and the pump was determined to be US$60. The average electricity rates for the cities were determined to be approximately 0.086 US$/kW-h (Tainan), 0.15 US$/kW-h (Madrid), 0.225 US$/kW-h (Osaka), 0.182 US$/kW-h (Hong Kong), and 0.253 US$/kW-h (Lisbon), and the average gas rates were 0.091 US$/kW-h (Tainan), 0.091 US$/kW-h (Madrid), 0.239 US$/kW-h (Osaka), 0.139 US$/kW-h (Hong Kong), and 0.118 US$/kW-h (Lisbon), listed in Table 9. The annual operating costs for the DHW systems in the five different locations were calculated using these values and the total electrical energy consumption for each system (Figs. 12–16). According to the results, the operating cost of the dual-tank system was determined to be lower than that of the single-tank system in all five locations.

Fig. 10 illustrates the payback periods relative to electrical heaters in the five cities. The payback period was calculated as follows:

$$\text{payback period} = \frac{|\text{Equipment cost of SDHW system} - \text{Equipment cost of conventional DHW system}|}{|\text{Operating cost of SDHW system} - \text{Operating cost of conventional DHW system}|} \quad (3)$$

Table 9
Electricity and gas costs in five cities.

Location	Electric price (USD/kW h)	Gas price (USD/kW h)
Taiwan (TW)	0.086	0.091
Madrid(ES)	0.150	0.091
Osaka(JP)	0.225	0.239
Hong Kong (CN)	0.182	0.139
Lisbon(PT)	0.253	0.118

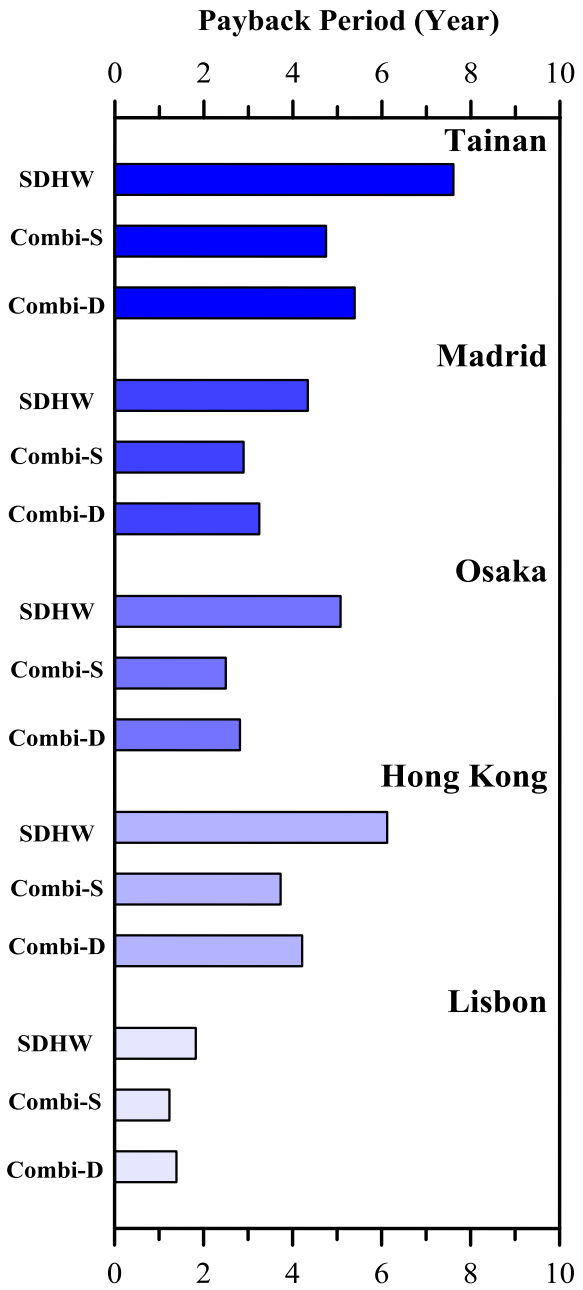

Fig. 10. Payback periods (relative to electric heaters) for three different types of domestic hot water systems in five cities.

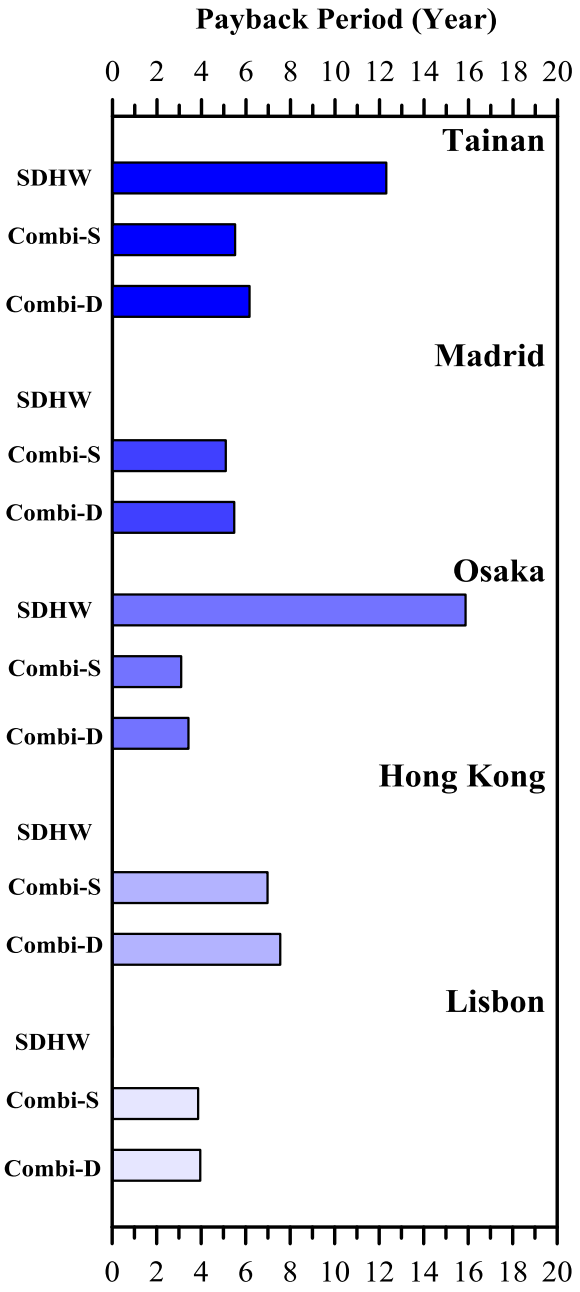

Fig. 11. Payback periods (relative to gas heaters) for three different types of domestic hot water systems in five cities.

Tainan was determined to have the longest payback period because the electricity price in Taiwan is lower than those of the other countries. Lisbon was determined to have the shortest payback period due to the higher electricity price and lower equipment cost. However, this calculation did not consider equipment depreciation rates, maintenance fees, or derivative expenses.

Fig. 11 illustrates the payback periods relative to gas-fired heaters in the five cities, although this is not applicable in locations where the operating cost and equipment cost of SDHW are higher than gas-fired heaters. Because the main heat source of an SDHW system is electrical, the electricity price is what matters, and lower electricity prices result in lower operating costs of SDHW systems. The payback periods for Tainan and Osaka were determined to be 12.3 and 15.9 years, respectively, because electricity is cheaper than gas in these locations. The payback period of the single-tank combisystem relative to gas-fired and electrical heaters in the different locations was the shortest (Figs. 10 and 11). Despite the lower operating cost of the dual-tank system, it was determined to have a longer payback period because of the capital outlay required for the additional equipment. The single-tank system therefore seems more economical; although the dual-tank system

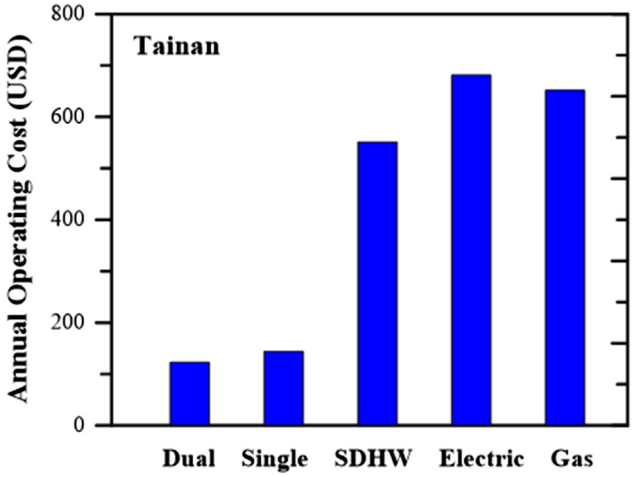

Fig. 12. Annual operating cost of each DHW system in Tainan.

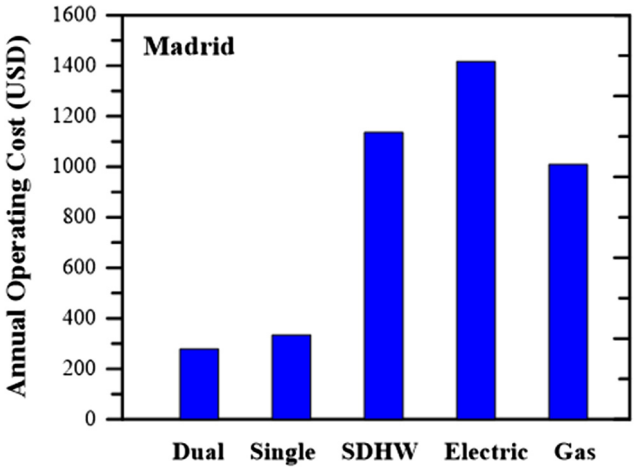

Fig. 13. Annual operating cost of each DHW system in Madrid.

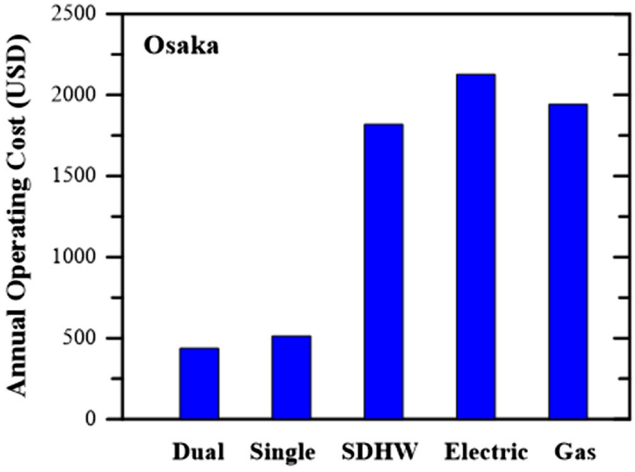

Fig. 14. Annual operating cost of each DHW system in Osaka.

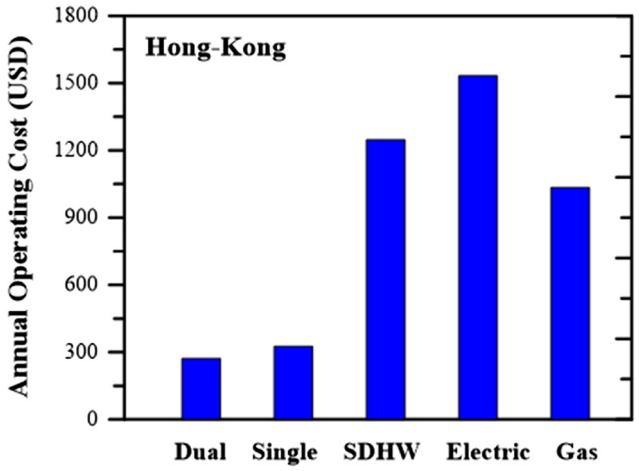

Fig. 15. Annual operating cost of each DHW system in Hong Kong.

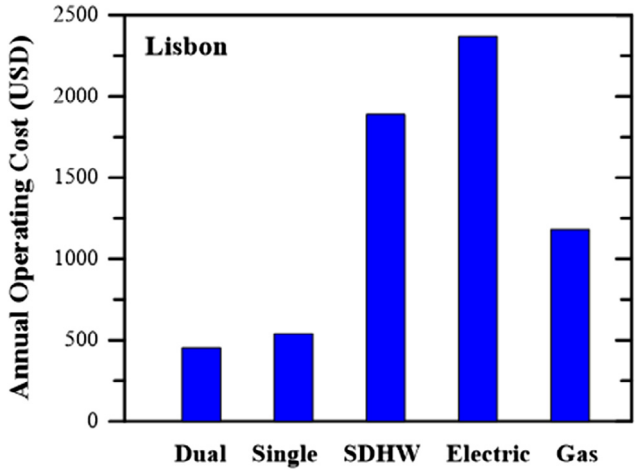

Fig. 16. Annual operating cost of each DHW system in Lisbon.

offers lower operating costs, the single-tank system has a shorter payback period. However, if the initial equipment cost can be reduced, the dual-tank system would become the optimal choice.

5. Conclusions

In this study, solar combisystems were analyzed through the Taguchi method under five different climatic conditions to determine their optimal operating parameters, the contribution of each parameter to performance, and the payback period. The results show that each parameter had a varying level of effect on performance in the different locations, and that this could be explained by the interplay between the climatic conditions and technical features of the SDHW systems in each considered city. Nevertheless, the most influential parameter was the same for all locations for each type of system. For the single-tank systems, the flow rate of the heat pump was most influential, but for the dual-tank system, it was the flow rate of the solar collector. This distinction arises because the single-tank system involves competition between the solar collector and the heat pump, but this does not apply to the dual-tank system.

The payback periods and operating costs in the five cities were also determined. The dual-tank system is more economical with regard to operating cost; however, the single-tank system offers a shorter payback period, because of the high initial equipment cost of the dual-tank system. If this initial cost of the dual-tank system could be reduced, it would be the optimal system, because the results of this study indicate that its design is more reliable across locations.

Acknowledgements

This research was partially supported by the Ministry of Science and Technology – Taiwan under Grant No. MOST 105-2628-E-006-005-MY3 and MOST 106-2923-E-006-003-MY3, and by the Bureau of Energy and Ministry of Economic Affairs, under Grant No. 105-D0303, Republic of China. Computer time and numerical packages provided by the Energy Research Center, National Cheng Kung University, Taiwan, are gratefully acknowledged.

References

[1] J.F. Chen, Y.J. Dai, R.Z. Wang, Experimental and theoretical study on a solar assisted CO2 heat pump for space heating, Renew. Energy 89 (2016) 295–304.
[2] G. Panaras, E. Mathioulakis, V. Belessiotis, A method for the dynamic testing and evaluation of the performance of combined solar thermal heat pump hot water systems, Appl. Energy 114 (2014) 124–134.
[3] S.R. Asaee, V.I. Ugursal, I. Beausoleil-Morrison, Techno-economic assessment of solar assisted heat pump system retrofit in the Canadian housing stock, Appl. Energy 190 (2017) 439–452.
[4] S.J. Sterling, M.R. Collins, Feasibility analysis of an indirect heat pump assisted solar domestic hot water system, Appl. Energy 93 (2012) 11–17.
[5] J. Cai, J. Ji, Y. Wang, W. Huang, Numerical simulation and experimental validation of indirect expansion solar-assisted multi-functional heat pump, Renew. Energy 93 (2016) 280–290.
[6] D. Carbonell, M.Y. Haller, D. Philippen, E. Frank, Simulations of combined solar thermal and heat pump systems for domestic hot water and space heating, Energy Proc. 48 (2014) 524–534.
[7] Y.H. Kuang, R.Z. Wang, Performance of a multi-functional direct-expansion solar assisted heat pump system, Sol. Energy 80 (7) (2006) 795–803.
[8] A. Galgaro, G. Emmi, A. Zarrella, M. De Carli, Possible applications of ground coupled heat pumps in high geothermal gradient zones, Energy Build. 79 (Suppl. C) (2014) 12–22.
[9] H. Lim, C. Kim, Y. Cho, M. Kim, Energy saving potentials from the application of heat pipes on geothermal heat pump system, Appl. Therm. Eng. 126 (Suppl. C) (2017) 1191–1198.
[10] S. Deng, Y.J. Dai, R.Z. Wang, Performance optimization and analysis of solar combi-system with carbon dioxide heat pump, Sol. Energy 98 (Part C) (2013) 212–225.
[11] G. Panaras, E. Mathioulakis, V. Belessiotis, Investigation of the performance of a combined solar thermal heat pump hot water system, Sol. Energy 93 (2013) 169–182.
[12] E. Bertram, Solar assisted heat pump systems with ground heat exchanger – simulation studies, Energy Proc. 48 (2014) 505–514.
[13] S. Qu, F. Ma, R. Ji, D. Wang, L. Yang, System design and energy performance of a solar heat pump heating system with dual-tank latent heat storage, Energy Build. 105 (2015) 294–301.
[14] W. Lerch, A. Heinz, R. Heimrath, Direct use of solar energy as heat source for a heat pump in comparison to a conventional parallel solar air heat pump system, Energy Build. 100 (2015) 34–42.
[15] Y. Liu, J. Ma, G. Zhou, C. Zhang, W. Wan, Performance of a solar air composite heat source heat pump system, Renewable Energy 87 (Part 3) (2016) 1053–1058.
[16] S. Poppi, C. Bales, A. Heinz, F. Hengel, D. Chèze, I. Mojic, C. Cialani, Analysis of system improvements in solar thermal and air source heat pump combisystems, Appl. Energy 173 (2016) 606–623.
[17] M. Jradi, C. Veje, B.N. Jørgensen, Performance analysis of a soil-based thermal energy storage system using solar-driven air-source heat pump for Danish buildings sector, Appl. Therm. Eng. 114 (2017) 360–373.
[18] F.M. Rad, A.S. Fung, W.H. Leong, Feasibility of combined solar thermal and ground source heat pump systems in cold climate Canada, Energy Build. 61 (2013) 224–232.
[19] S. Awani, S. Kooli, R. Chargui, A. Guizani, Numerical and experimental study of a closed loop for ground heat exchanger coupled with heat pump system and a solar collector for heating a glass greenhouse in north of Tunisia, Int. J. Refrig 76 (2017) 328–341.
[20] C. Tzivanidis, E. Bellos, G. Mitsopoulos, K.A. Antonopoulos, A. Delis, Energetic and financial evaluation of a solar assisted heat pump heating system with other usual heating systems in Athens, Appl. Therm. Eng. 106 (2016) 87–97.
[21] J. Zhu, D. Li, S. Zhao, Study on application of solar water heat pump for building in China, Proc. Eng. 121 (2015) 1200–1207.
[22] T.T. Chow, G. Pei, K.F. Fong, Z. Lin, A.L.S. Chan, M. He, Modeling and application of direct-expansion solar-assisted heat pump for water heating in subtropical Hong Kong, Appl. Energy 87 (2) (2010) 643–649.

[23] H. Esen, E. Turgut, Optimization of operating parameters of a ground coupled heat pump system by Taguchi method, Energy Build. 107 (2015) 329–334.
[24] T. Sivasakthivel, K. Murugesan, H.R. Thomas, Optimization of operating parameters of ground source heat pump system for space heating and cooling by Taguchi method and utility concept, Appl. Energy 116 (2014) 76–85.
[25] V. Verma, K. Murugesan, Optimization of solar assisted ground source heat pump system for space heating application by Taguchi method and utility concept, Energy Build. 82 (2014) 296–309.
[26] TRNSYS, A Transient System Simulation Program: V17.01.0025., Solar Energy Lab, University of Wisconsin-Madison, USA, 2012
[27] Y.-H. Li, W.-C. Kao, Performance analysis and economic assessment of solar thermal and heat pump combisystems for subtropical and tropical region, Sol. Energy 153 (2017) 301–316.
[28] S. Poppi, C. Bales, M.Y. Haller, A. Heinz, Influence of boundary conditions and component size on electricity demand in solar thermal and heat pump combisystems, Applied Energy 162 (2016) 1062–1073.
[29] S. Deng, Y.J. Dai, R.Z. Wang, Performance optimization and analysis of solar combi-system with carbon dioxide heat pump, Solar Energy 98 (2013) 212–225, Part C.